J. Basic. Appl. Chem., 7(1)9-25, 2017

ISSN 2090-424X
Journal of Basic and Applied Chemistry
www.textroad.com

Corrosion Protection of Tin in 1M HCl by Expired Primperan and E-mox Drugs-Part I

E. M. Attia, N. S. Hassan and A. M. Hyba

Chemistry Department, Faculty of Science (Girls), Al-Azhar University, Nasr city, Cairo, Egypt.

ABSTRACT

The protective properties of expired Primperan (EPD) and E-mox (EMD) drugs were scrutinized as inhibitors for tin corrosion in 1M HCl. The study was performed in different concentrations of expired drugs (0-9% (v/v)) and at different temperatures (20 – 60 °C). Open circuit potential and potentiodynamic techniques were used in the experimental methods. The functional groups presented in the expired drugs after transient expiration date was investigated by infra-red (IR) analysis. Scanning electron microscope (SEM) analysis was used to illustrate the morphology of the surface. Open circuit potential and potentiodynamic polarization measurements demonstrated that by increasing inhibitors concentrations and decreasing temperature, the inhibition efficiency increased. Potentiodynamic measurements showed that the process of adsorption was of physical type and act upon Temkin's adsorption isotherm at all studied temperatures. Calculation and discussion of the activation energy (E_a), enthalpy (ΔH°_{ads}), entropy (ΔS°_{ads}) and free energy of adsorption (ΔG°_{ads}) were included.

KEYWORDS: Expired drugs, Tin, Corrosion, Inhibitor, Polarization, IR, SEM.

1. INTRODUCTION

Hundreds of industrial processes were performed using tin metal especially when alloyed with different elements. Bronze and solder are common alloys which produced from tin metal. In the aerospace industry, tin is alloyed with titanium and it is also used as an ingredient in some insecticides [1]. Different tin compounds can be used to provide semiconducting properties. For example, tin sulfide film, was formed by potentiostatic anodic polarization of tin in aqueous electrolyte containing sulfide ions. The surface film exhibits semiconducting properties and bilayer structure with the p–type conductivity representing the inner layer which consists of Sn(II) sulfide and n–type conductivity representing the outer layer which consists of Sn(IV) sulfide [2]. Zhou *et al*. [3] showed that the corrosion rate of tinplate may be reduced by adding inhibitors, or by adjusting the pH and temperature, removing dissolved oxygen or lowering the conductivity of the electrolyte. Concerning addition of inhibitors, researchers were looking for the environmentally friendly, non-toxic and cheap corrosion inhibitors. Recently, drugs are reported environmentally friendly and important in biological reactions (i.e. non-hazardous).

When most drugs pass their expiry date, they are generally become unsuitable for human health use. Some researchers [4-9] tested expired drugs as corrosion inhibitors, where the active constituent destroys only infinitesimally. It was proved by Food and Drug Administration (FDA) that; after the expiration dates, 90% of the drugs are unchanging for elongated period [10]. The high molecular weight of drugs and easily solubility in water, together with the presence of hetero atoms in their structure compromises possible inhibition to the corrosion process[11].

Therefore, the aim of the present work is to examine the inhibitive effect of two expired drugs, which in their valid state had active ingredients containing two different types of amides; an aromatic amide and a cyclic amide for expired Primpran (EPD) and E- mox (EMD) respectively. The study was performed on tin electrode in 1M HCl solution using open circuit potential and potentiodynamic polarization methods at different temperatures.

2. MATERIALS AND METHODS

2.1. Electrode preparation:-

A rod of tin with the chemical composition (wt %): 0.013 Fe; 0.400 Si; 0.780 Ti and 97.500 Sn; was used as the working electrode. A circular surface area of 2.27 cm² was exposed to contact the electrolyte. The polishing of the surface was done using emery papers ranging from 800 to 1200 grit. The surface was then washed with distilled water, degreased in acetone and finally dried in a soft cloth.

2.2. Aggressive solution:-

The aggressive 1M HCl solution was prepared by dilution of AR reagent grade 37% concentrated acid using bi-distilled water at 25 °C.

***Corresponding Author**: E. M. Attia, Chemistry Department, Faculty of Science (Girls), Al-Azhar University, Nasr city, Cairo, Egypt.

2.3. Inhibitors

Primperan (syrup) is an Egyptian drug produced by SANOFI AVENTS Co. The empirical formula of metoclopramide, the active ingredient of Primperan syrup, is $C_{14}H_{22}ClN_3O_2$, with molecular weight being 299.8 g/mol and melting point being 147.3 °C. The systematic (IUPAC) name of metoclopramide is 4-amino-5-chloro-N-(2-(diethylamino) ethyl)- 2-methoxybenzamide, and its molecular structure is represented in Figure (1). The expired Primperan drug (EPD) was tested as inhibitor.

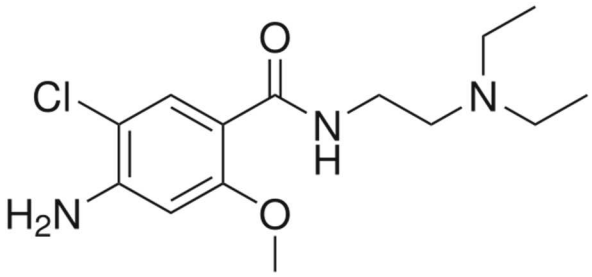

Figure 1: Molecular structure of metoclopramide.

E-mox syrup is an antibacterial drug penicillin family produced by EIPICO Company. It is a β-lactam derivative (four- membered cyclic amide). Each 5ml of drug contains 250 mg of amoxicillin, the active ingredient of E-mox syrup. The empirical formula of amoxicillin is $C_{16}H_{19}N_3O_5S$, with molecular weight being 365.4 g/mol and melting point being 194 °C. The systematic (IUPAC) name of amoxicillin is (2S, 5R, 6R)-6-{[(2R)-2-amino-2-(4-hydroxyphenyl)-acetyl] amino}-3, 3-dimethyl-7-oxo-4-thia-1-azabicyclo [3.2.0] heptane-24-carboxylic acid and its molecular structure is represented in Figure (2). The expired E-mox drug (EMD) was tested as inhibitor.

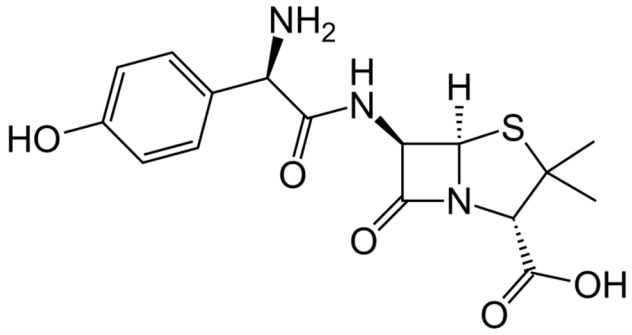

Figure 2: Molecular structure of amoxicillin.

2.4. Experimental Methods

2.4.1. Infrared analysis

IR analysis in this work was used to determine details about the functional groups that still present after passing expiration date in expired drugs molecules which can be revealed by analyzing the spectrum of absorbed frequencies.

2.4.2. Open circuit potential

The measurements of open-circuit potentials were performed in a glass cell of 25ml capacity for 150 min relating to a saturated calomel electrode (SCE). The working tin electrode was immersed in the cell vertically and the potentials were recorded as a function of time till establishing of steady state values using digital multimeter (Keithley, Model 175, USA).

2.4.3. Potentiodynamic polarization measurements:-

An Electronic Potentioscan Wenking (Model POS 73) was used to produce potentiodynamic polarization measurements. The measurements were done in a glass cell comprising three openings for electrodes. One opening was for the reference electrode (SCE), the second for the auxiliary platinum sheet (2 cm^2) and the third one for the working tin electrode. The E– log I plots for all solutions were swept from -2 to +2 V/SCE at scan rate 2 mVs^{-1}. The working electrode was first immersed into the test solution for 150 min to reach a quasi-stationary value of the open circuit potential prior to the measurements.

The corrosion rate (C_R) in mpy, was calculated using Eq.1[8,9]:

$$C_R = 0.13 \times \mathrm{I_{corr}} \times e/d \qquad (1)$$

where 0.13 is the metric and time conversion factor, I_{corr} is the corrosion current density in μA/cm², e and d are the equivalent weight and density of metal in geq/mol and g/cm³ respectively. Values of I_{corr} and corrosion potential (E_{corr}) were evaluated from intersection of the linear anodic and cathodic branches of Tafel plots. Degrees of surface coverage (θ) in potentiodynamic measurements were calculated using Eq. 2.

$$\theta = \left[1 - \frac{I_{corr}}{I^{\circ}_{corr}}\right] \qquad (2)$$

where I°_{corr} and I_{corr} are the corrosion current densities in absence and presence of inhibitors, respectively. Each experiment was repeated three times at least.

2.4.4. Surface characterization:-

The surface morphologies of tin samples were studied by using scanning electron microscope (SEM). The scanning tests were performed on abraded samples and on samples after exposer for 2h to 1M HCl in the absence and presence of expired drugs at 20 °C.

3. RESULTS AND DISCUSSION

3.1. Infra-Red analysis

Figure 3 (a and b) represents the IR spectrum of metoclopramide and EPD respectively. In metoclopramide (Figure 3-a), the vibration bands due to (NH_2) group disappeared in the spectrum of expired drug (Figure 3-b). In Metoclopramide spectrum, a band of amide group appeared at 1200 cm^{-1} became broad and shifted to 1600 cm^{-1} after expiration. The IR spectrum of EPD also illustrated a broad band due to N-H at 3448 cm^{-1}, bands due to C=C at 2016 cm^{-1}, aromatic C-H at 2000 cm^{-1} , C=O at 1650 cm^{-1} and C-N at 1620 cm^{-1}.

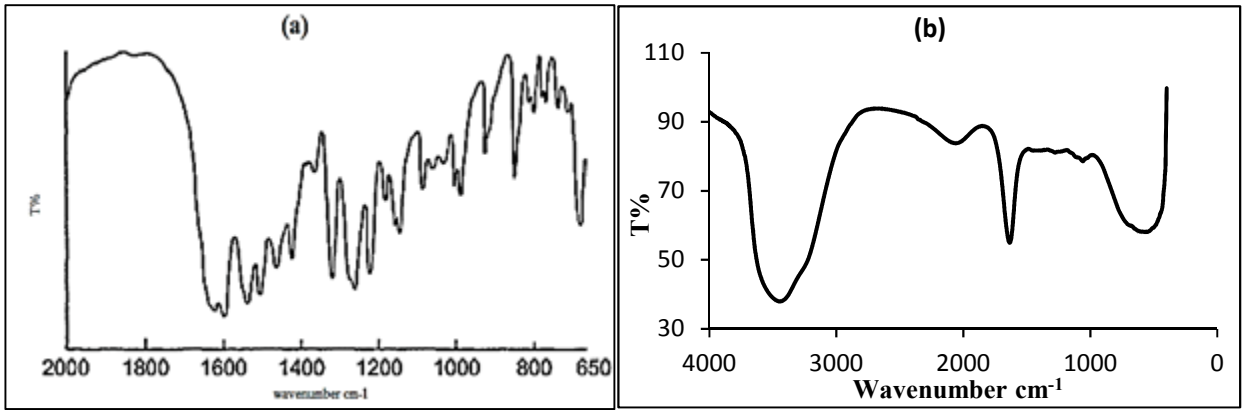

Figure 3: IR spectrum of Metoclopramide (a) and EPD (b).

Figure (4-a) represented the spectrum of amoxicillin, before getting expired. The stretching vibration mode characteristic for ν(NH_2) at 3300 and 3350 cm^{-1} for amoxicillin sample were disappeared in the spectrum of the EMD (Figure 4-b). The stretching vibration band of ν(OH) group in amoxicillin sample at 3200 cm^{-1} became very broad in the EMD sample. Additionally, weak C-N band at ≈1500 cm^{-1} and C=C at 1624 cm^{-1} were detected in EMD sample. The bands due to ν(C=O) and ν(C-S-C) moiety at 1600 and 700 cm^{-1} were disappeared in the expired drug sample. All the charts of IR spectrum were analyzed according to Stuart [12].

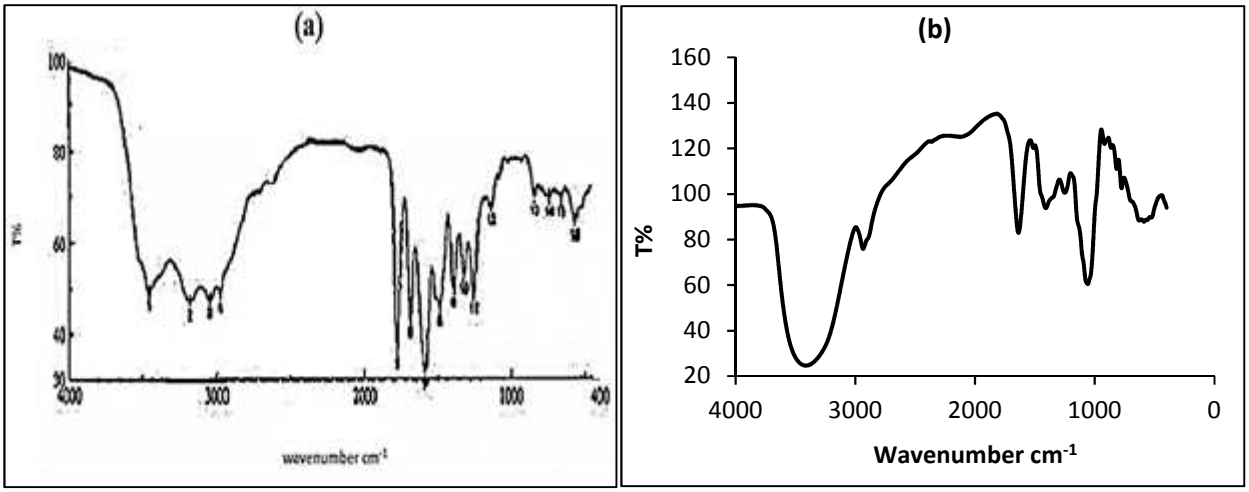

Figure 4: IR spectrum of Amoxicillin (a) and EMD (b).

3.2. Open Circuit Potential Measurements (OCP)

3.2.1. Effect of immersion time:-

The open circuit potential-time behavior of tin electrode at 20 °C in absence and presence of 9% of EPD and EMD was recorded and shown in Figure 5. The behavior of tin electrode in presence of expired drugs was similar to that in blank solution (1M HCl), where the curves moved downwards in blank and inhibited solutions. The potential– time curves for the two tested inhibitors were characterized by three portions; the first one exhibited a general tendency for the immersion open-circuit potential to shift sharply from less negative to more negative values (corrosion process) at the first two minutes of immersion. This might be attributed to the damage of pre-immersion air formed oxide film presented on the tin surface in the acidic solutions [13]. In the second portion of the curves (continued up to 60 min), the potential got more negative with increasing time in a lower rate. In the third region, the potential remained almost constant for a long period of time which led to the steady state potential values [14]. The steady state portion may be ascribed to the development of stannic oxide (SnO_2) above the surface, which increases the resistance of anodic area which leads to passivation [15]. Similar behaviors were recorded at temperature range from 30 to 60 °C.

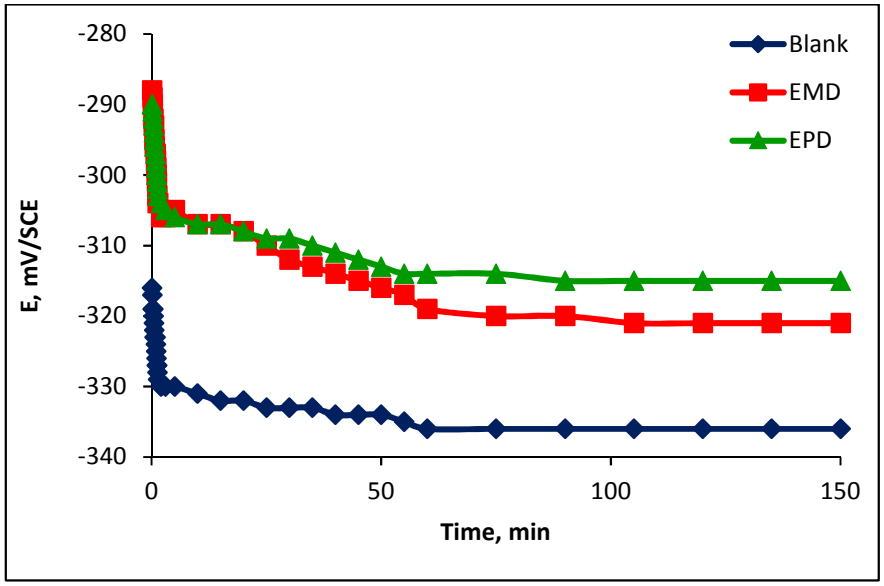

Figure 5: Variation of the open-circuit potential for tin electrode in 9% of EMD and EPD at 20 °C.

3.2.2. Effect of inhibitor concentration:-

Figure 6 illustrated that (at 20 °C) the potential of tin electrode in blank solution was more negative than that in the acid solutions containing different concentrations of the two expired drugs. It is also observed that, by increasing the concentration of the two expired drugs in 1M HCl solution, the potentials got less negative. The dependence of open circuit potential on concentration was very marked. This suggested that the expired drugs molecules were powerfully and quickly adsorbed at the steady state potentials [16].

In all concentrations for the two expired drugs, the immersion and steady state potential values were in negative side of the hydrogen/hydrogen ion electrode system. This might indicate that the nature of the cathodic reaction occurring at the electrode surface was mainly hydrogen ion discharge and the depolarization effect of oxygen was less manifested.

The curves of Figure (6) showed that EPD and EMD were effective in retarding the corrosion process because these additives shifted the potential towards less negative values. This might be attributable to the adsorption of the expired drugs on an oxide-free tin surface and delaying the hydrogen evolution reaction at the cathodic sites. The inhibition increased the protection qualities of the oxide surface or other surface layer from the aggressive solutions. The fundamental step involved displacement of pre-adsorbed water molecules by the inhibitors followed by electrostatic interaction at the surface [14]. Figure (6) also illustrated that by increasing the concentration of inhibitors, the steady state potential of tin shifted towards less negative values. This meant that the equilibrium state established between film dissolution and formation shifted towards the formation process at greater inhibitor concentrations [17]. This behavior was observed at all temperature range and the details of immersion and steady state potential values were illustrated in Tables 1 and 2.

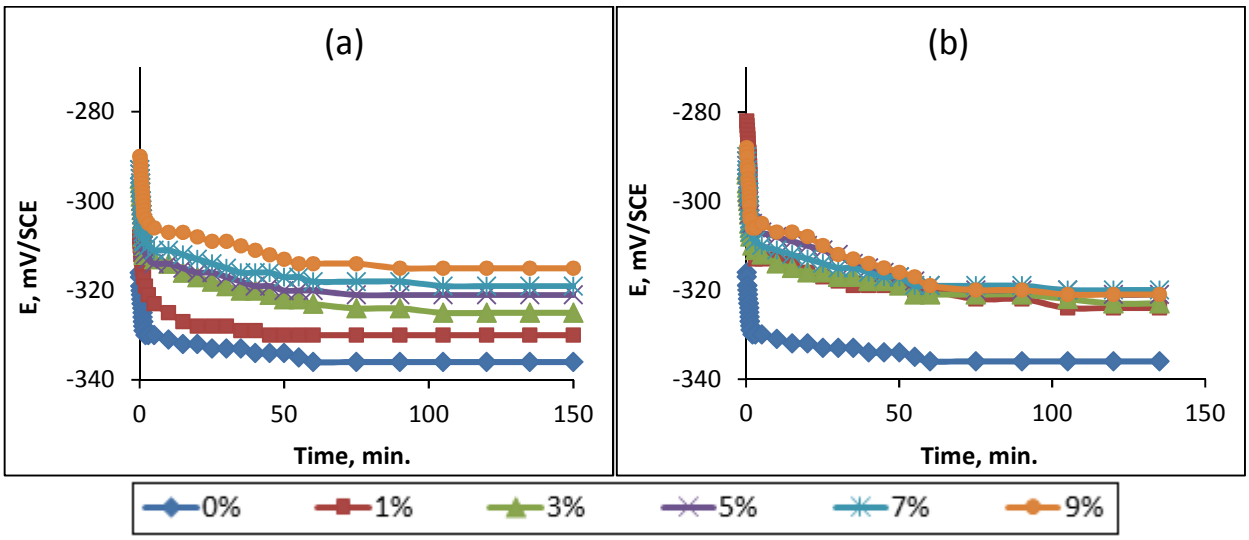

Figure 6: Variation of the open-circuit potential for tin electrode in different concentrations of (a) EPD and (b) EMD at 20 °C.

3.2.3. Effect of temperature:-

The curves of Figure 7-a illustrated that the immersion potential of tin electrode, at 9% EPD, were increased and decreased in a random manner by increasing the temperature. Concerning tin in 9% EMD, the immersion potentials were decreased regularly with increasing temperature. The immersion potential of tin electrode was higher in EMD than in EPD at 20, 40 and 60 °C.

Regarding the temperature effect on the steady state potentials (E_{ss}), Figure 7-b illustrated that, tin in presence of 9% EPD showed equal E_{ss} values at 30 and 40 °C which were lower than that recorded at 20 and 50 °C and higher than that recorded at 60 °C. On the other hand, tin immersed in 9% EMD had decreasing E_{ss} values with increasing temperature. The steady state potential of tin electrode was higher in EMD than in EPD at 30, 40 and 60 °C. For blank solutions, increasing the temperature was conjugated with decreasing both of E_{imm} and E_{ss} values.

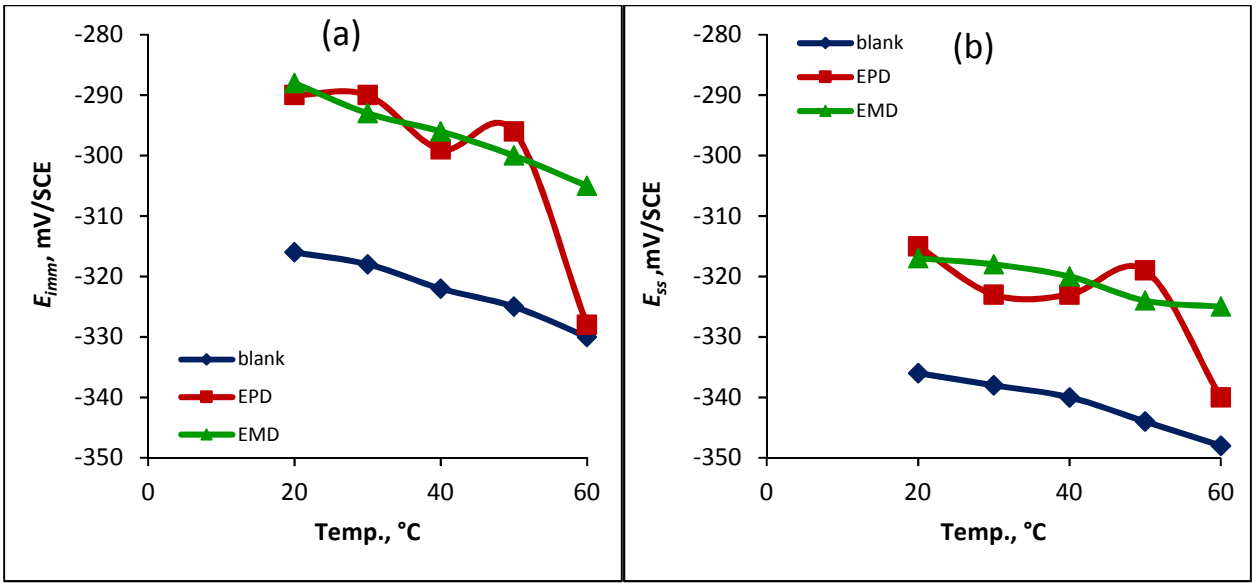

Figure 7: Variation of the (a) immersion and (b) steady state potentials for tin electrode in 9% of EPD and EMD compared with blank solution at different temperatures.

3.2.4. Dissolution rates of pre- formed film on tin electrode:-

As the rate of a chemical reaction is defined as the decrease in the reactant concentration with time, in OCP technique, the rate of metal dissolution may be represented graphically as a linear relation between the drops in the electrode potential with respect to time. Figure (8) demonstrated the variation of the potentials, with the logarithm of the immersion time of tested inhibitors which represented mathematically by Eq. 3:

$$E = \alpha - b \log t \quad (3)$$

Where α is the pre-immersion film thickness, it depends on the composition of electrolyte and its concentration and temperature. The negative sign indicates the dissolution of the pre-immersion film; b is the slope of the straight line which represents the dissolution rate.

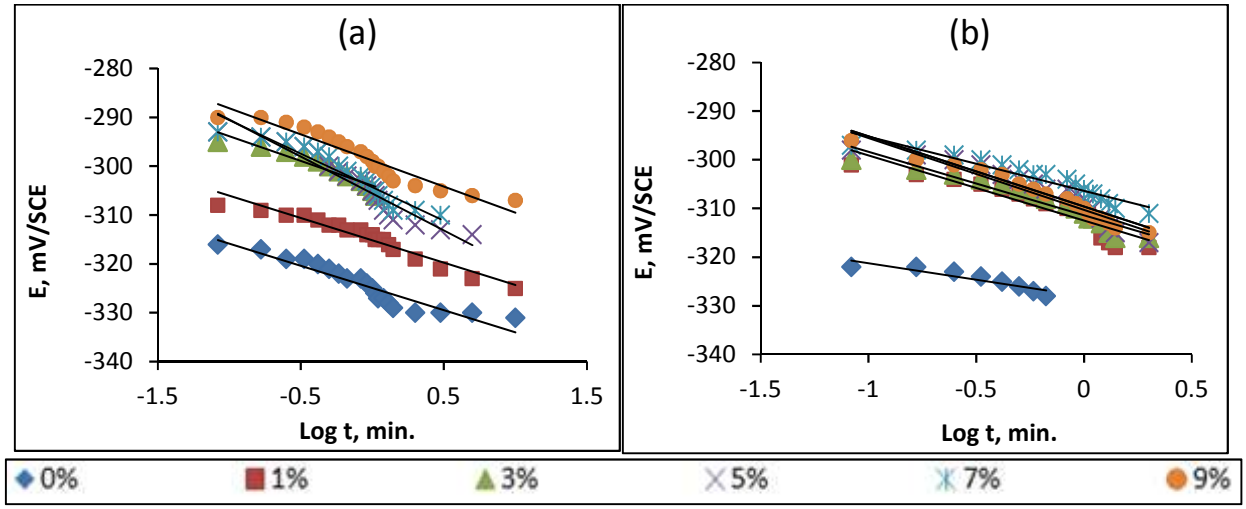

Figure 8: E-log t plots of tin electrode in absence and presence of different concentration of (a) EPD and (b) EMD at 20 ºC.

Values of calculated slopes and α with linearity coefficient (R^2) at temperature range 20 – 60 °C were recorded in Tables 1 and 2. The slopes of the linear relations changed with changing the type of expired drug. It ranges from -2.9 to -18.2 mV/decade for EPD and from 5 to -16.3 mV/decade for EMD. The most negative slope value indicated faster rate for electrode dissolution. It was also observed that there was no regular relation among slope values and concentrations or temperatures for the two expired drugs.

Generally α taken less negative potential values with the increase in the concentrations of EPD and EMD. At 60 °C, α had the most negative values at all concentrations. Addition of 1% of EMD to the blank solution at all temperatures raised the magnitude of α by average values of 20 mV. Increasing the concentrations of EMD to 3, 5, 7 and 9% had slight changeable values than that recorded at 1% (v/v).

Table 1: OCP parameters of tin electrode in 1M HCl in absence and presence of different concentration of EPD at temperature range of 20- 60 °C

Temp. °C	Conc., %(v/v)	E_{imm} mV/SCE	E_{ss} mV/SCE	Slopes	α	R^2
	0	-316	-336	-9.09	-325	0.8926
	1	-308	-330	-9.16	-315	0.9433
	3	-295	-325	-10.11	-304	0.9094
20	5	-293	-321	-15.11	-306	0.9171
	7	-293	-319	-13.72	-304	0.9117
	9	-290	-315	-10.69	-299	0.9151
	0	-318	-338	-10.19	-327	0.8987
	1	-308	-330	-9.16	-315	0.9433
	3	-300	-325	-18.21	-306	0.8766
30	5	-293	-324	-11.04	-303	0.9805
	7	-292	-329	-8.99	-308	0.9136
	9	-290	-323	-8.83	-299	0.9779
	0	-322	-340	-6.29	-328	0.8431
	1	-308	-335	-11.30	-319	0.9205
	3	-302	-332	-4.28	-306	0.9343
40	5	-301	-330	-3.69	-304	0.8222
	7	-299	-329	-5.38	-304	0.9127
	9	-299	-323	-2.79	-302	0.8638
	0	-325	-344	-17.19	-331	0.8907
	1	-327	-340	-4.73	-332	0.9015
	3	-305	-337	-9.39	-313	0.9032
50	5	-305	-336	-14.92	-317	0.8819
	7	-297	-323	-3.65	-300	0.8043
	9	-296	-319	-4.87	-298	0.7178
	0	-330	-348	-8.57	-338	0.9440
	1	-338	-363	-10.03	-346	0.9708
	3	-333	-355	-5.47	-338	0.8962
60	5	-325	-350	-11.63	-334	0.9152
	7	-312	-346	-4.50	-316	0.8962
	9	-328	-340	-2.91	-331	0.8788

Table 2: OCP parameters of tin electrode in 1M HCl in absence and presence of different concentration of EMD at temperature range of 20- 60 ºC

Temp. °C	Conc., %(v/v)	E_{imm} mV/SCE	E_{ss} mV/SCE	Slopes	α	R²
	0	-316	-336	-9.09	-325	0.8926
	1	-294	-324	-6.32	-295	0.8214
	3	-293	-323	-12.25	-304	0.9314
20	5	-291	-321	-10.37	-301	0.8936
	7	-290	-320	-13.21	-301	0.8857
	9	-288	-317	-14.33	-300	0.9097
	0	-318	-338	-10.19	-327	0.8987
	1	-299	-326	-10.71	-309	0.9347
	3	-298	-324	-11.66	-308	0.8720
30	5	-295	-323	-11.56	-306	0.9071
	7	-295	-321	-10.78	-305	0.9317
	9	-293	-318	-10.75	-303	0.8991
	0	-322	-340	-6.80	-328	0.8431
	1	-301	-328	-13.35	-312	0.8624
	3	-300	-326	-13.03	-311	0.9182
40	5	-298	-325	-14.44	-310	0.8662
	7	-297	-322	-11.16	-306	0.9135
	9	-296	-320	-14.74	-310	0.9632
	0	-325	-344	-17.19	-331	0.8907
	1	-305	-329	-10.88	-314	0.9410
	3	-303	-328	-11.26	-313	0.9140
50	5	-301	-326	-10.79	-310	0.9425
	7	-300	-325	-11.26	-310	0.9235
	9	-300	-324	-10.54	-309	0.9319
	0	-330	-348	-8.57	-338	0.944
	1	-312	-330	-5.08	-317	0.8932
	3	-311	-329	-8.54	-318	0.8927
60	5	-309	-328	-8.20	-317	0.9831
	7	-308	-326	-6.90	-314	0.9457
	9	-305	-325	-6.69	-308	0.8789

5.3. Potentidynamic polarization measurements:-

5.3.1. Effect of inhibitor concentration:-

Potentiodynamic polarization curves for tin in 1M HCl solution, free and comprising different concentrations of expired drugs at 20 ºC are shown in Figure (9). The respective potentiodynamic parameters covering corrosion potential (E_{corr}), corrosion current density (I_{corr}), anodic (β_a) and cathodic (β_c) Tafel slopes, the degree of surface coverage (θ), inhibition efficiency of inhibitor (IE%) and corrosion rates (C_R), for the two tested expired drugs are listed in Tables 3 and 4.

Studying carefully the curves of Figure (9); we can conclude that both EPD and EMD perform as mixed inhibitors. This was based on the observed shift detected on both cathodic and anodic branches of the curves compared with the blank solution [18].

The main anodic reactions in presence of Cl^- ions are shown below:[8, 19-22].

$$Sn \rightarrow Sn^{2+} + 2e^- \quad (4)$$

$$Sn^{2+} \rightarrow Sn^{4+} + 2e^- \quad (5)$$

$$2H_2O \rightarrow 4H^+ + O_2 + 4e^- \quad (6)$$

$$2Cl^- \rightarrow Cl_2 + 2e^- \quad (7)$$

The main cathodic reactions are:

$$2H_2O + 2e^- \rightarrow H_2 + 2OH^- \quad (8)$$

$$O_2 + 2H_2O + 4e^- \rightarrow 4OH^- \quad (9)$$

The highly insoluble $Sn(OH)_4$ will form according to reactions (10) or (11)

$$Sn + 4H_2O \rightarrow Sn(OH)_4 + 4H^+ + 4e^- \quad (10)$$

$$Sn^{4+} + 4H_2O \rightarrow Sn(OH)_4 + 4H^+ \quad (11)$$

The conversion of $Sn(OH)_4$ to SnO_2 included free energy change ~ −42 kJ mol^{-1} [23]. So that, the strength of the passive layer improved with its irreversible dehydration to SnO_2, according to reaction (12) [23, 24].

$$Sn(OH)_4 \rightarrow SnO_2.H_2O + H_2O \qquad (12)$$

In the existence of inhibitors particles, and when the surface was fully roofed with $Sn(OH)_4$ and/or $SnO_2.H_2O$ film, the active places on the surface would be obstructed and the corrosion current sent down to a slight value, indicating the beginning of passivation [8].

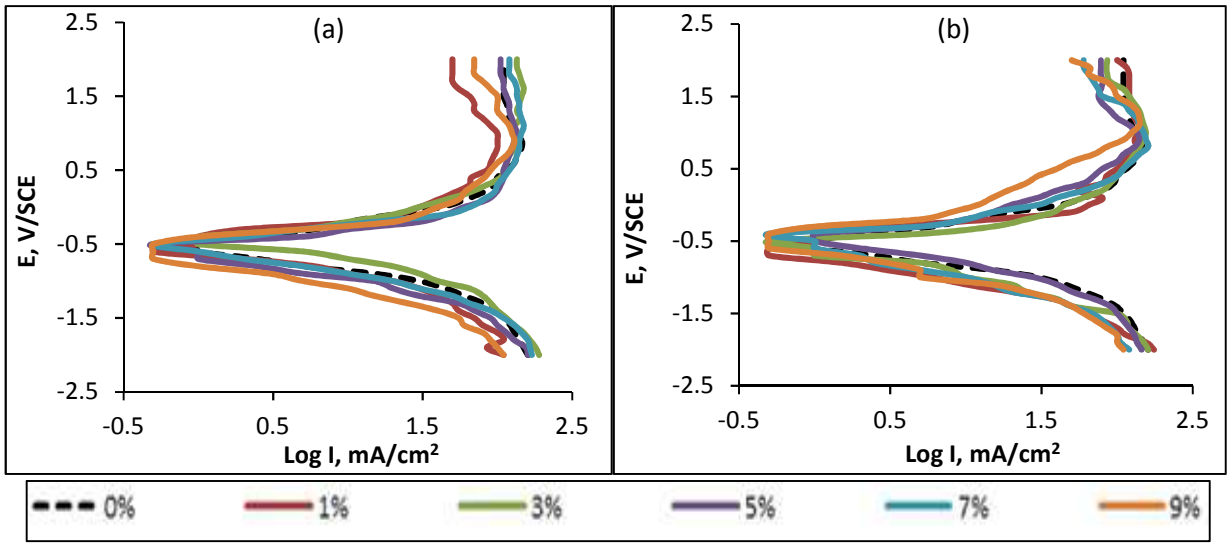

Figure 9: Polarization plots of tin in 1M HCl in absence and presence of different concentrations of (a) EPD and (b) EMD at 20 °C.

Table 3: Potentiodynamic parameters for tin electrode in different concentrations of EPD at temperatures range of 20- 60 °C

Temp. °C	Conc., %(v/v)	E_{corr}, mV/SCE	I_{corr}, mA/cm²	C_R, mpy	β_a, mV/dec	- β_c mV/dec	θ	IE%
20	0	-550	50.1	52903	2000	1000	-	-
	1	-550	6.3	6660	769	833	0.8741	87.41
	3	-520	5.0	5290	588	1000	0.8999	89.99
	5	-510	4.5	4714	400	2500	0.9108	91.08
	7	-500	3.2	3337	400	2000	0.9369	93.69
	9	-500	1.8	1877	500	1666	0.9645	96.45
30	0	-600	63.1	66605	1000	1000	-	-
	1	-600	14.3	15046	2000	769	0.7741	77.41
	3	-590	13.5	13279	714	588	0.7866	78.66
	5	-580	8.7	9180	555	666	0.8621	86.22
	7	-570	6.9	7330	588	500	0.8899	89.00
	9	-550	3.7	3924	555	666	0.9401	94.11
40	0	-450	66.1	69740	1428	666	-	-
	1	-630	18.5	19516	1250	1250	0.7201	72.01
	3	-620	12.6	13288	1000	1000	0.8094	80.94
	5	-600	10.0	10555	769	769	0.8486	84.86
	7	-590	7.9	8384	714	714	0.8797	87.97
	9	-570	5.0	5290	500	500	0.9241	92.41
50	0	-400	70.8	74733	1666	833	-	-
	1	-650	20.9	22054	769	1666	0.7049	70.49
	3	-630	15.9	16733	125	1111	0.7761	77.61
	5	-620	12.0	12705	769	1000	0.8300	83.00
	7	-600	10.0	10560	833	588	0.8587	85.87
	9	-590	6.3	6666	769	200	0.9108	91.08
60	0	-400	112.2	118433	10000	1250	-	-
	1	-670	34.8	36714	1250	1250	0.6900	69.00
	3	-650	27.4	28886	500	1428	0.7761	75.61
	5	-630	20.0	21061	833	1250	0.8221	82.21
	7	-610	19.0	20134	769	1000	0.8300	83.00
	9	-600	12.3	13028	1000	500	0.8900	89.00

Table 4: Potentiodynamic parameters for tin electrode in different concentrations of EMD at temperatures range of 20- 60 °C

Temp. °C	Conc., %(v/v)	E_{corr}, mV/SCE	I_{corr}, mA/cm^2	C_R, mpy	β_a, mV/dec	- β_c mV/dec	θ	IE%
20	0	-550	50.1	52903	2000	1000	-	-
	1	-540	10.0	10555	1000	1250	0.8004	80.04
	3	-530	7.9	8384	769	2000	0.8415	84.15
	5	-550	6.3	6660	769	2000	0.8741	87.41
	7	-520	5.6	5936	769	2500	0.8877	88.77
	9	-510	4.0	4202	769	1666	0.9205	92.05
30	0	-600	63.1	66605	1000	1000	-	-
	1	-670	15.8	16729	1250	769	0.7488	74.88
	3	-620	12.6	13288	1000	666	0.8004	80.04
	5	-590	10.0	10555	769	1250	0.8415	84.15
	7	-650	7.9	8384	1000	588	0.8741	87.41
	9	-630	6.3	6660	666	714	0.8999	89.99
40	0	-450	66.1	69740	1428	666	-	-
	1	-500	20.0	21061	2000	666	0.6980	69.80
	3	-500	15.8	16729	1000	625	0.7601	76.01
	5	-520	10.6	13288	1000	714	0.8394	83.94
	7	-520	8.7	10555	400	909	0.8686	86.86
	9	-450	8.3	8384	1000	714	0.8797	87.41
50	0	-400	70.8	74733	1666	833	-	-
	1	-400	25.1	26514	1666	434	0.6452	64.52
	3	-480	20.0	21061	1428	333	0.7181	71.81
	5	-480	12.6	13288	1250	500	0.8221	82.21
	7	-475	10.6	10555	769	625	0.8300	83.00
	9	-480	9.9	9407	769	555	0.8500	85.00
60	0	-400	112.2	118433	1000	1250	-	-
	1	-400	41.6	43962	909	588	0.6288	62.88
	3	-390	33.0	34802	1666	666	0.7061	70.61
	5	-350	28.9	30548	1250	434	0.7420	74.20
	7	-380	20.0	21081	1000	555	0.8220	82.20
	9	-480	18.0	18947	1000	714	0.8400	84.00

According to previous studies; (i) if the displacement in E_{corr} is > 85mV with respect to the recorded values of blank solution, the inhibitor can be classified as a cathodic or anodic type, (ii) if displacement in E_{corr} is < 85, the inhibitor can be classified as mixed type [25].

From Table 3, it can be seen that EPD behaved as mixed type inhibitor at 20 and 30 °C, while behaved as cathodic inhibitor at 40, 50 and 60 °C. For EMD (Table 4), the maximum displacement was less than 85 mV at all conditions, indicating that it was a mixed type inhibitor. Tables (3 and 4) also illustrated that there were an observable decrement in the corrosion current densities and consequently on the corrosion rates accompanying the increase in concentration of the two expired drugs at all temperatures. The high values of Tafel slopes were due to surface kinetic process instead of diffusion-controlled process [26]. Some anomalous values of Tafel slopes may be originated from various mechanisms of metal dissolution, depending on the type of electrolyte. This behavior may be due to that some part of the applied voltage was consumed across the oxide and was hence not available to support the charge transport at the electrode/solution interface. There was a barrier within the oxide film that moderated the passage of electrons through the film and submission of higher overvoltage was necessary for the reaction to occur [27]. The degree of both surface coverage and inhibition efficiency increased with increasing the inhibitor concentration. This indicated that the tested expired drugs performed as good inhibitors for tin corrosion in 1M HCl media [28].

5.3.2. Effect of temperature:-

Referring to Tables (3 and 4), positive correlation was observed between temperature and corrosion current densities and corrosion rates in inhibited and especially in uninhibited solutions which confirmed the potentially of using these expired drugs as corrosion inhibitors. In presence of inhibitors, however, at high temperatures, the expired drugs dissociated to produce more destructive ions causing higher corrosion rates than expected. The transference of the adsorption– desorption equilibrium in the direction of desorption was the main reason for the observed decrease in the surface coverage and the inhibition efficiencies that tracked the increase in temperature. Such behavior suggested that investigated EPD and EMD were physically adsorbed on the tin surface [29]. Abd El-Maksoud [30] explain the reason for this behavior as follows; by increasing the temperature, the break between adsorption and desorption of inhibitors became shorter. This leaves the metal surface bare for extended time in the corrosive solution. Thus higher corrosion rates and lower IE% are expected at higher temperatures [31].

5.3.3. Kinetic and thermodynamic corrosion parameters:-

The relation between corrosion rate and temperature was illustrated by Arrhenius (Equation 13) and was represented graphically in Figure 10.

$$\log C_R = A - (E_a/2.303\,RT) \qquad (13)$$

where A is the extrapolation factor, E_a is the activation energy, R is the universal gas constant and T is the absolute temperature. A plot of $\log C_R$ vs. $1/T$ gives straight line with slope $E_a/2.303$ R (from which E_a can be calculated) and the intercept is the constant A. The enthalpy ΔH^* and entropy ΔS^* of activation for the corrosion process were calculated using the Eyring transition state (Equation 14).

$$\log C_R/T = \log(R/Nh) + (\Delta S^*/2.303R) - (\Delta H^*/2.303RT) \qquad (14)$$

Where N is Avogadro's number, h is the Planck's constant, ΔS^* is the entropy change of activation and ΔH^* is the enthalpy change of activation. Straight lines representing the relation between $\log C_R/T$ against $1/T$ were obtained in Figure 11. From slopes of $(-\Delta H^*/2.303R)$ and intercepts of $[\log(R/Nh) + (\Delta S^*/2.303R)]$, the values of ΔH^* and ΔS^* were calculated and given in Table 5.

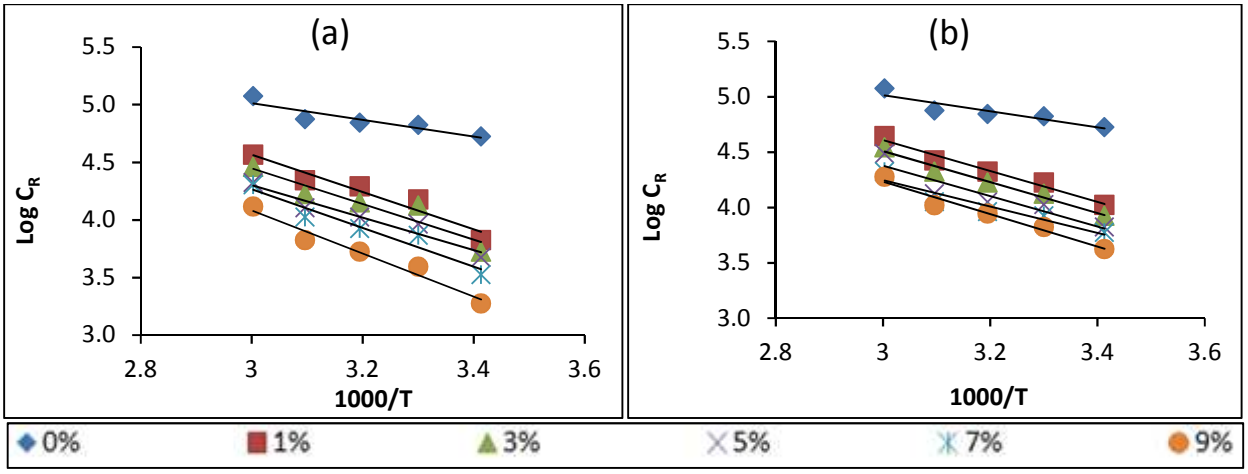

Figure 10: Arrhenius plots for Sn in absence and presence of different concentrations of (a) EPD and (b) EMD.

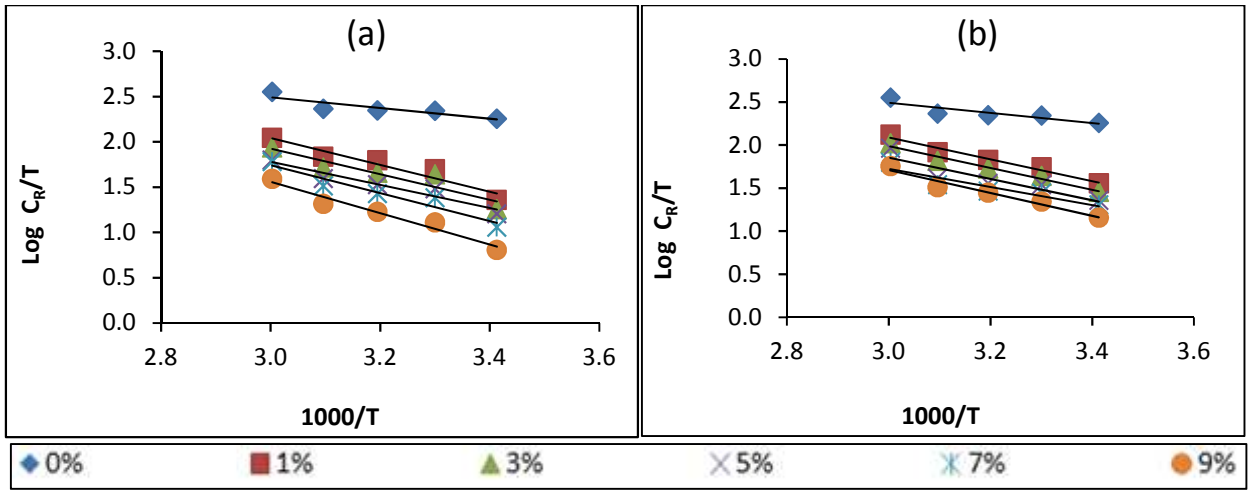

Figure 11: Eyring transition state plots for Sn in absence and presence of different concentrations of (a) EPD and (b) EMD.

Table 5: Activation energy and Eyring thermodynamic parameters for tin electrode in different concentrations of EPD and EMD

Expired Drug	Conc. %(v/v)	E_a KJ/mol	ΔH^* KJ/mol	ΔS^* J/molK
Blank	0	13.90	11.30	-173.40
	1	30.98	28.39	-73.29
	3	29.58	26.99	-79.76
EPD	5	26.98	24.39	-90.36
	7	32.16	29.56	-75.51
	9	35.77	33.17	-68.19
	1	26.84	24.25	-84.86
	3	26.79	24.20	-86.95
EMD	5	26.35	23.76	-90.78
	7	22.73	20.14	-104.17
	9	28.04	25.45	-88.49

The higher values for E_a and ΔH^* produced in the presence of EPD or EMD compared with the blank solution (Table 5) indicated the increase in the height of the energy barrier of the corrosion reaction which decreased with increasing temperature [29, 32]. The significant difference between these values and the value for the blank solution indicated that EPD and EMD retarded effectively the corrosion of tin in 1M HCl solution.

It was also noted from Table 5 that in presence of EPD or EMD, E_a was greater than 20 kJ/mol and lower than 40 kJ/mol, hence the entire process was controlled by surface reaction [33]. The positive ΔH^* values in all types of solutions indicated the endothermic nature of the activation process which suggested its difficult and slow dissolution in presence of expired drugs [34]. The values of ΔS^* in the absence and presence of EPD or EMD had large and negative values. This indicated that a decrease in disordering took place on going from reactants to activated complex [35].

5.3.4. Temkin adsorption isotherm and thermodynamic adsorption parameters:-

The experimental data for expired drugs, best fitted the Temkin isotherm. The degree of fitting was determined by applying the regression coefficient (R^2). Equation 15 characterizes the mathematical representation of the isotherm.

$$\theta = \frac{-2.303 \operatorname{Log} K_{ads}}{2a} - \frac{2.303 \operatorname{Log} C}{2a} \qquad (15)$$

Where θ is the degree of surface coverage, K_{ads} is the adsorption equilibrium constant and C is the inhibitor concentration. Values of the parameter (a), is considered as a measure for the sharpness of the adsorption isotherm. The Temkin adsorption isotherm was represented graphically in Figure 12 by plotting (θ) against (Log C), the adsorption parameters were listed in Table (6).

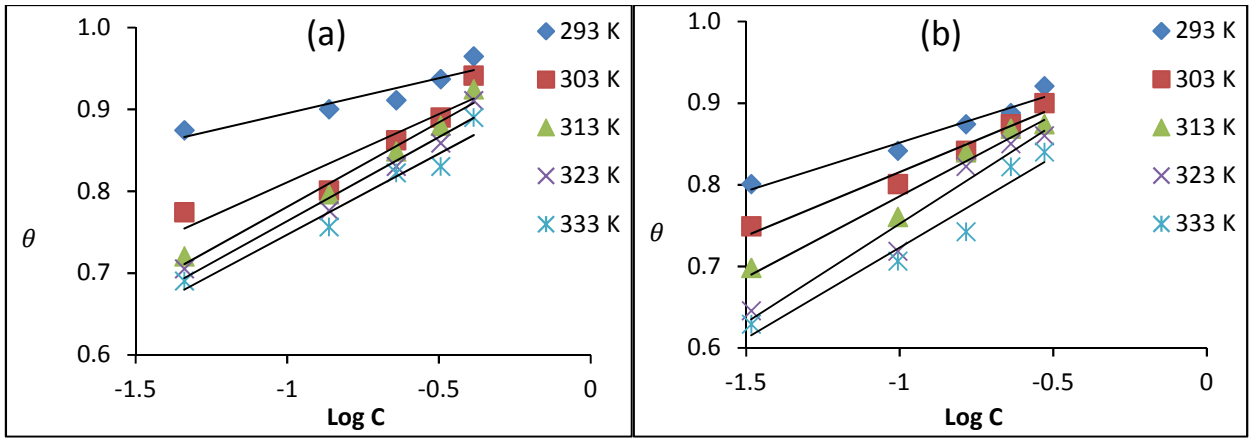

Figure 12: Temkin adsorption isotherm for (a) EPD and (b) EMD at different temperatures.

Table 6: Temkin adsorption parameters of tin in 1M HCl containing EPD and EMD at different temperatures

Expired Drug	Temp. °C	*a*	K_{ads} mol^{-1}	R^2
	20	-13.4	8.43E+05	0.8711
	30	-6.9	7.43E+05	0.8699
EPD	**40**	-5.5	6.16E+04	0.9759
	50	-5.6	6.01E+04	0.9623
	60	-5.8	5.29E+04	0.9491
	20	-9.7	1.48E+08	0.9581
	30	-7.4	1.65E+06	0.9682
EMD	**40**	-5.8	9.06E+04	0.9603
	50	-4.8	1.27E+04	0.9539
	60	-5.2	1.79E+04	0.9417

The spontaneity of the adsorption process was ensured by the negative values of "a" [36]. The adsorptive equilibrium constant (K_{ads}) for the two expired drugs indicated that, with rising the temperature, the force that binds the inhibitors molecules to the metal surface decreased. This behavior was ideal for tin in EPD, while in EMD an exception was observed at 60 °C in which tin had higher K_{ads} values than that recorded at 50 °C.

Such behavior of decreasing K_{ads} with increasing temperature was due to the easily adsorption of inhibitors molecules on the tin surface at lower temperatures. On the contrary, rising the temperature facilitates desorption of some molecules of the expired drugs from the tin surface. Generally, large values of K_{ads} were bound up with more efficient adsorption. This means that the double-layer formed between the outer layer of the surface and the adsorbed inhibitor molecules has strong electrical interaction [36, 37]. The equilibrium constant of adsorption (K_{ads}) was related to the standard free energy of adsorption (ΔG_{ads}) using Equation 16.

$$K_{ads} = (1/55.5) \exp -(\Delta G^{\circ}_{ads}/RT) \qquad (16)$$

The heat of adsorption was evaluated by using the Gibbs- Helmholtz equation (Equation 17), which represented graphically in Figure 13. Values of ΔG°_{ads} and ΔH°_{ads} were listed in Table (7).

$$\frac{\Delta G^{\circ}_{ads}}{T} = \frac{\Delta H^{\circ}_{ads}}{T} + K \qquad (17)$$

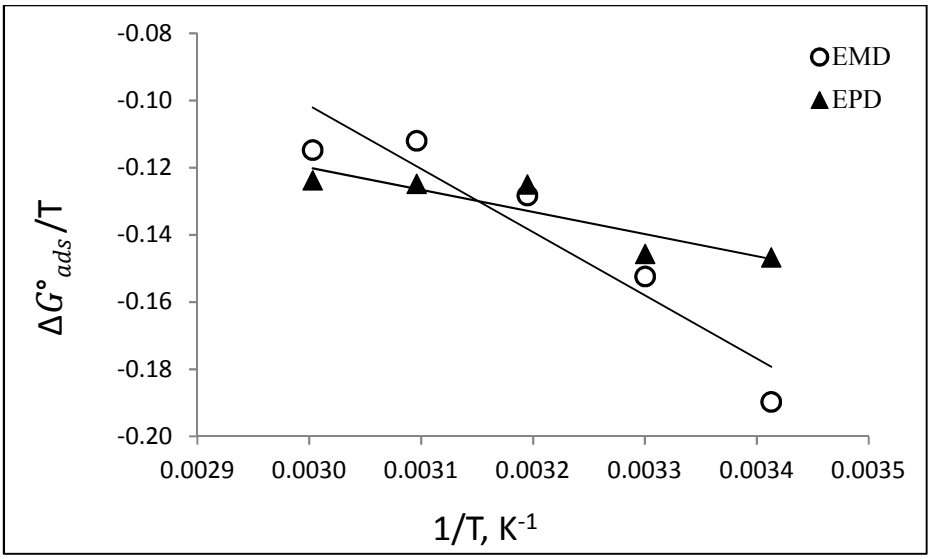

Figure 13: Gibbs-Helmholtz's plot of EPD and EMD.

As shown from Table 7, the calculated values of ΔG°_{ads} for tin electrode in the presence of EPD and EMD were all more negative than -35 kJ/mol. This signifies stability of the spontaneous adsorbed layer [38] and that both physical and chemical adsorption process was involved [39]. But returning to Tables 3 and 4, the observed decrease in the inhibition efficiency followed increasing the temperature indicated the predominantly physical adsorption on the tin surface. On the other hand the negative values of ΔH°_{ads} for the two expired drugs revealed an exothermic adsorption process.

The entropy of adsorption (ΔS°_{ads}), was calculated using Equation 18, and the values were tabulated in Table 7.

$$\Delta S^{\circ}_{ads} = \frac{\Delta H^{\circ}_{ads} - \Delta G^{\circ}_{ads}}{T} \qquad (18)$$

It is known that when the process agreed with an exothermic adsorption process; this followed by a lower entropy values and vice versa [29]. Table (7) illustrated that EMD provided more negative entropy values at all temperatures than EPD indicating exothermic adsorption process in the both tested inhibitors.

Table 7: Thermodynamic adsorption parameters of tin in 1M HCl containing EPD and EMD at different temperatures

Expired Drug	Temp. °C	ΔG°_{ads} kJ/mol	ΔH°_{ads} kJ/mol	ΔS°_{ads} KJ/molK
	20	-43		-0.08
	30	-44		-0.07
EPD	**40**	-39	-66	-0.09
	50	-40		-0.08
	60	-41		-0.07
	20	-56		-0.45
	30	-46		-0.47
EMD	**40**	-40	-188	-0.47
	50	-36		-0.47
	60	-38		-0.45

5.5.1.1. Scanning electron microscopic study (SEM):-

Figure (14-a) showed the initial surface state of tin prior to exposure, a clean surface with no corrosion products but only some nicks were observed on the surface of tin. It was also observed that some fine scratches resulting from the grounding progress are visible in the images.

After 2h of exposure to blank solution (1M HCl), disappearance of the original nicks was evidence of anodic dissolution of Sn. The tin surface became fractured; coarse and permeable due to its coverage with corrosion products layers which were inhomogeneous and imperfect (Figure 14-b). The fractures in the tin surface represent anodic positions at which dissolution occurs and spread by increasing the contact time.

The immersion of Sn metal in 1M HCl solution containing 1% EPD for 2h resulted in the formation of uneven sides and loosely spread film on the Sn surface (Figure 14-c). In the presence of 1% EMD (Figure 14-d), the aggressive action of HCl reduced obviously, confirming the effective inhibition action at this low concentration.

Figure 14-e showed that the particle layers progressively grew thicker in presence of 9% EPD which lost their uneven sides observed in 1% concentration and became ragged with closed structures. The surface morphology of tin in 9% EMD (Figure 14-f) was better than that in 1% EMD (Figure 14-d).

Thus, at 9% concentration, the produced films became homogenous and perfect with better protective performance for tin electrode. Therefore, with increasing expired drug concentration, the corrosion rate of tin decreased. These results were consistent with those of OCP and potentiodynamic polarization measurements.

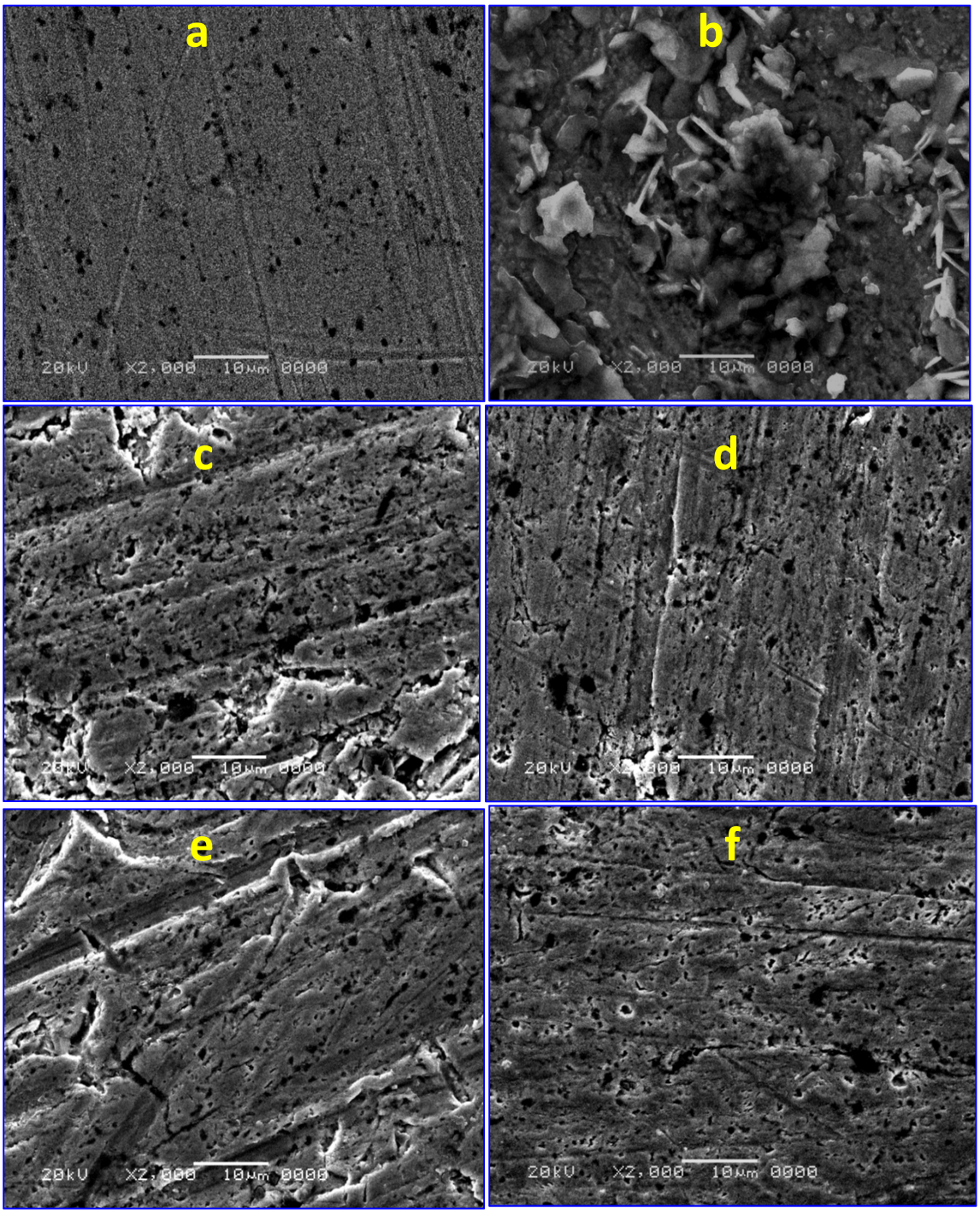

Figure 14: SEM micrograph for Sn coupons (a) Abraded Sn; (b) Sn in 1M HCl; (c) Sn in 1% EPD; (d) Sn in 1% EMD; (e) Sn in 9% EPD; (f) Sn in 9% EMD at 20 °C.

Mechanism of adsorption

The IR spectrum of EPD (Figure 3-b) illustrated presence of the following bands: C=O, N–H, C=C and Ar C–H. Instead, it illustrated disappearance of $–NH_2$ group. Thus, the existence of Cl^- which is electron donating atom, and also the presence of unshared electron pairs in the atoms of O and N, and π-electrons of aromatic ring are the main reasons for the inhibition of tin in presence of EPD. Similarly the inhibition action in presence of EMD was due to the presence of unshared electron pairs in the atoms of O and N but not through the π electrons of the ring since IR spectrum (Figure 4-b) illustrated the presence of O–H and C–N bonds whereas there is no evidence about the presence of aromatic ring due to expiration effect.

However, the present ingredient can be protonated in HCl solution. They become cations, existing in equilibrium with the corresponding molecular forms. On the other hand the negative chloride ions adsorb onto the positively charged tin surface, changing the surface negatively charged. To balance the polarities on the tin interface, the protonated species migrate to the tin surface permitting the electrostatic attraction. This process allows physical adsorption onto the tin surface, and thereby giving high inhibition by expired drugs molecules.

CONCLUSION

1. From OCP and potentiodynamic polarization measurements, the corrosion of Sn in 1M HCl solutions was retarded in the presence of EPD and EMD and the effect of EPD was better than EMD.
2. EPD behaved as mixed type inhibitor at 20 and 30 ^oC, while behaved as cathodic inhibitor at 40, 50 and 60 ^oC.
3. EMD behave as mixed inhibitors at all concentrations and temperatures.
4. The inhibition efficiency increased with increasing inhibitor concentration but decreased with increasing temperature.
5. The adsorption of EPD and EMD followed the Temkin's adsorption isotherm.
6. The process of adsorption was spontaneous and exothermic and of physical type.
7. The dissolution of tin was of endothermic nature, accompanied by increase in the system ordering.

REFERENCES

1- S.C. Britton and D.G. Michael, J. Appl. Chem. 7 (7) (1957) 349-356.
2- J. Katić, M. Metikoš-Huković, I. Šarić and M. Petravić, J. Electrochem. Soc. 164(7) (2017) 383-389.
3- D. Zhou, J. Wang, Y. Gao and L. Zhang, Int. J. Electrochem. Sci., 12 (2017) 192-205.
4- R.S. Abdel Hameed, journal of physical chemistry, PCAIJ, 8(4) (2013) 146-149.
5- H.I. Al-Shafey, R.S. Abdel Hameed, F.A. Ali, A.S. Aboul-Magd and M. Salah, Int. J. Pharm. Sci. Rev. Res., 27(1) (2014) 146-152.
6- A.M. El-Desoky, H.M. Ahmed and A.E. Ali, Int. J. Electrochem. Sci., 10 (2015) 5112-5129.
7- E.M. Attia, J. Basic. Appl. Chem., 5(1) (2015) 1-15.
8- E.M. Attia, N.S. Hassan and A.M. Hyba, Int. J. Adv. Res. 4(2) (2016) 872-886.
9- E.M. Attia, N.S. Hassan and A.M. Hyba, J. Basic. Appl. Chem., in press.
10- N. Vaszilcsin, V. Ordodi and A. Borza, Int. J. Pharm., 431 (2012) 241-244.
11- P. Geethamani, P.K. Kasthuri and S. Aejitha, Int. J. Chem. Pharm. Sci., 3(1) (2015) 1442-1448.
12- B. Stuart, Infrared Spectroscopy: Fundamentals and Applications, John Wiley and Sons, (2004).
13- A.N. Smith, Int. J. Electrochem. Sci., 9 (2014) 6006-6019.
14- R.M. Abou Shahba, A.S.I. Ahmed, E.M. Attia and A.E. EL- Shennawy, Al-Azhar Bull. Sci., 19 (1) (2008) 269-281.
15- C.W. Wagner and W. Traud, Electrochem. Soc., 44(1938) 391-454.
16- R.S. Abdel Hameed, E.A. Ismail, A.H. Abu- Nawwas and H.I. AL-Shafey, Int. J. Electrochem. Sci., 10 (2015) 2098-2109.
17- M.M. El-Rabiee, N.H. Helal, Gh.M. Abd El-Hafez and W.A. Badawy, J. Alloys and Compounds, 459 (2008) 466-471.
18- G. Golestani, M. Shahidi and D. Ghazanfari, Appl. Surf. Sci., 308 (2014) 347-362.
19- S.S. Abd El Rehim, H.H. Hassan and N.F. Mohamed, Corros. Sci., 46 (2004) 1071-1082.
20- S.B. Lyon, Corrosion of Tin and its Alloys. Shreir's Corrosion, T.J.A. Richard- son, Ed., Elsevier, New York, (2010) 2068-2077.
21- R.M. El-Sherif, and W.A. Badawy, Int. J. Electrochem. Sci., 6 (2011) 6469- 6482.

22- B. Liao, L. Wei, Z. Chen and X. Guo, RSC Adv., 7(2017) 15060-15070.
23- S.S. Abd El Rehim, H.H. Hassan and N.F. Mohamed, Corros. Sci., 46 (2004) 1071-1082.
24- H.H. Hassan and K. Fahmy, Int. J. Electrochem. Sci., 3 (2008) 29-43.
25- S.H. Kumar, S. Karthikeyan, S. Narayanan and K.N. Srinivasan, Int. J. Chem. Tech. Research, 4(3) (2012) 1077-1084.
26- A.M. El-Desoky, H.M. Ahmed and A.E. Ali, Int. J. Electrochem. Sci., 10 (2015) 5112-5129.
27- I. Mickova, A. Prusi, T. Grcev and L. Arsov, Croat. Chem. Acta, 79(4) (2006) 527-532.
28- K.Z. Mohammed and M. Abbas, J. Pharm. Bio. Chem. Sci., 3(2) (2012) 912.
29- A.S. Fouda and H.E. Gadow, GJRE: Chem. Eng., 14(2) (2014) 22-36.
30- S.A. Abd El-Maksoud, Int. J. Electrochem. Sci., 3(2008) 529.
31- M.M. Solomon, S.A. Umoren, I.I. Udosoro and A.P. Udoh, Corros. Sci., 52 (2010) 1317-1325.
32- A.S. Fouda, H.A. Mostafa, and H.M. El-Abbasy, J. Appl. Electrochem., 40(1) (2010) 163-173.
33- A.S. Fouda, F.E. Heakal and M.S. Radwan, J. Appl. Electrochem., 39(3) (2009) 391-402.
34- A.S. Fouda, S.A. Abdel-Maksoud, and A.E. Almetwally, Chem. Sci. Transact., 4(1) (2015) 161-175.
35- E.M. Attia, Int. J. Adv. Res. 4(3) (2016) 986-1003.
36- A.S. Fouda, A.M. El-Defrawy, and M.W. El-Sherbeni, J. Electrochem. Sci. Tech., 4(2) (2013) 47-56.
37- A. Ansari, M. Znini, I. Hamdani, L. Majidi, A. Bouyanzer, and B. Hammouti, J. Mate. Envi. Sci., 5(1) (2014) 81-94.
38- I.B. Obot, E.E. Ebenso and M.M. Kabanda, J. Envi. Chem. Engi., 1(2013) 431-439.
39- J.I. Bhat and V.D.P. Alva, Scholars Research Library Archives of Applied Science Research, 3(1) (2011) 343-356.